

Adaptive Exploration for Latent-State Bandits

Jikai Jin*
 jkjin@stanford.edu
 The Institute for Computational and
 Mathematical Engineering
 Stanford University
 Stanford, California, USA

Baoyi Shi
 baoyis@meta.com
 Central Applied Science
 Meta
 Menlo Park, California, USA

Kenneth Hung
 kenhung@meta.com
 Central Applied Science
 Meta
 Menlo Park, California, USA

Sanath Kumar Krishnamurthy
 sanathsk@meta.com
 Ranking AI Research
 Meta
 Menlo Park, California, USA

Congshan Zhang
 cszhang@meta.com
 Central Applied Science
 Meta
 Menlo Park, California, USA

Abstract

The multi-armed bandit problem is a core framework for sequential decision-making under uncertainty, but classical algorithms often fail in environments with hidden, time-varying states that confound reward estimation and optimal action selection. We address key challenges arising from unobserved confounders, such as biased reward estimates and limited state information, by introducing a family of state-model-free bandit algorithms that leverage lagged contextual features and coordinated probing strategies. These implicitly track latent states and disambiguate state-dependent reward patterns. Our methods and their adaptive variants can learn optimal policies without explicit state modeling, combining computational efficiency with robust adaptation to non-stationary rewards. Empirical results across diverse settings demonstrate superior performance over classical approaches, and we provide practical recommendations for algorithm selection in real-world applications.

CCS Concepts

- Computing methodologies → Online learning settings; Causal reasoning and diagnostics;
- Mathematics of computing → Markov processes.

Keywords

Contextual bandit, Non-stationary bandit, Confounding variables, Causal inference

ACM Reference Format:

Jikai Jin, Kenneth Hung, Sanath Kumar Krishnamurthy, Baoyi Shi, and Congshan Zhang. 2026. Adaptive Exploration for Latent-State Bandits. In *Proceedings of XXX (XXX '26)*. ACM, New York, NY, USA, 11 pages. <https://doi.org/XXXXXX.XXXXXXX>

*Work done during internship at Central Applied Science, Meta

Permission to make digital or hard copies of all or part of this work for personal or classroom use is granted without fee provided that copies are not made or distributed for profit or commercial advantage and that copies bear this notice and the full citation on the first page. Copyrights for components of this work owned by others than the author(s) must be honored. Abstracting with credit is permitted. To copy otherwise, or republish, to post on servers or to redistribute to lists, requires prior specific permission and/or a fee. Request permissions from permissions@acm.org.

XXX '26, XXX, XXX

© 2026 Copyright held by the owner/author(s). Publication rights licensed to ACM. ACM ISBN XXX-X-XXXX-XXXX-X/XXXX/XX
<https://doi.org/XXXXXX.XXXXXXX>

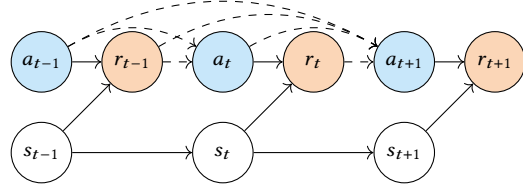


Figure 1: A directed acyclic graph (DAG) representing the causal relationship among hidden state s_t , action a_t and reward r_t . The solid arrows represent the latent-state bandit setting we have, while the dashed arrows represent the feedback from past actions and rewards due to the bandit algorithm.

1 Introduction

The multi-armed bandit problem is a fundamental framework for sequential decision-making with applications in online advertising [11], recommendation systems [30], clinical trials [13], and resource allocation [20]. While classical bandit algorithms assume that reward distributions are either constant or depend only on observable contextual features, many real-world scenarios are better considered as *non-stationary bandit problems*. Specifically, we consider here hidden time-varying states that (1) significantly influence the action-reward mapping, (2) transition autonomously with no influence from the action taken, but (3) remain unobservable to the decision-maker. These states create a challenging setting where optimal actions that maximize the instantaneous reward depend on latent environmental conditions that must be inferred from historical observations. Figure 1 shows a directed acyclic graph to illustrate the relationship among the hidden states, actions and rewards

As a motivating example, consider an online advertising platform that must repeatedly select which ad to display. While the platform observes user demographics and browsing history, it cannot directly observe broad environmental variables (e.g., the weather) or the user's current cognitive state (e.g., whether they are focused or distracted, browsing casually or ready to purchase). These hidden states critically influence ad effectiveness and evolve over time: a user might transition from "browsing" to "purchase-ready", or their attention might fluctuate based on the weather. An algorithm that

ignores these latent dynamics will misestimate ad performance and make suboptimal decisions.

This scenario exemplifies a fundamental limitation of traditional contextual bandit algorithms: they either ignore dependencies on these hidden states entirely, or require explicit state observations that are unavailable in practice. This leads to *systematic confounding*, where the algorithm’s reward estimates are biased by unobserved factors, resulting in sub-optimal long-term performance.

1.1 Key Challenges

The presence of unobserved time-varying confounders creates three fundamental challenges:

- (1) Confounded reward estimation: Standard bandit algorithms estimate arm values by averaging observed rewards, but when rewards depend on hidden states, these estimates reflect a mixture over state distributions rather than state-conditional values. This leads to systematic bias when the optimal action varies across states — standard algorithms will converge to an arm that is mediocre in all states but optimal in none.
- (2) Temporal reward attribution: When rewards depend on hidden states that evolve over time, observed performance changes may result from either learning progress or state transitions. Disentangling these effects complicates the exploration-exploitation trade-off: a seemingly obvious improvement might simply reflect a favorable state, while genuine learning progress might be masked by an unfavorable state transition.
- (3) Limited state information: Unlike fully observable contextual bandits, algorithms cannot directly condition on state information and must rely on indirect signals to infer the current state. This task becomes increasingly difficult as the state space grows.

1.2 Our Contributions

Our key insight is that hidden states, while not directly observable, leave observable traces in reward sequences, and these traces can be extracted through carefully designed contextual features and exploration strategies.

We develop a family of *state-model-free* bandit algorithms that learn optimal policies without explicitly estimating the hidden state space. Our approach combines two complementary strategies:

- (1) Lagged contextual learning: Previous rewards and actions serve as informative proxies for hidden states. Our **Lagged-context UCB (LC-UCB)** algorithm treats the action-reward pair (r_{t-1}, a_{t-1}) as contextual features, enabling implicit state tracking via observable interaction history.
- (2) Coordinated probing: Motivated by an arm identification issue of LC-UCB (see Example 1), we develop probing strategies that generate contextual signals by regularly exploring different arms in coordinated patterns. This strategy reveals cross-arm relationships and reward structures that would remain hidden under LC-UCB. We introduce **Randomized Probing UCB (RP-UCB)** for settings with multiple experimental units that can be simultaneously assigned different arms, **Sequential Probing UCB (SP-UCB)** for single-unit settings, using sequential arm sampling.

Naturally, one can combine these two complementary approaches to achieve the best of both worlds: temporal context extraction provides continuous state tracking capabilities, while coordinated exploration generates the rich joint information needed to disambiguate state-dependent reward patterns. Along this line, we develop an adaptive probing scheme that allows the algorithm to determine when intensive exploration is most beneficial, leading to **Adaptive Randomized Probing UCB (AdaRP-UCB)** and **Adaptive Sequential Probing UCB (AdaSP-UCB)**.

Notably, all these approaches require no state model: rather than attempting to explicitly model potentially exponential hidden state spaces and estimate the states, we learn optimal policies by constructing informative feature representations. This approach combines the computational efficiency of classical bandit algorithms with the adaptive capacity needed for non-stationary rewards.

We conduct systematic empirical evaluation across parameter sweeps — varying the number of hidden states, environmental volatility, reward noise, and time horizons. Our algorithms consistently outperform classical methods for standard, adversarial and non-stationary bandits, with particularly strong performance in complex environments where continuous and timely adaptation is crucial. Based on our experimental findings, we also provide practical guidance for choosing the best algorithm in different real-world scenarios.

1.3 Related Work

Classical and Contextual Bandits. The multi-armed bandit problem, introduced by Robbins [35], includes foundational algorithms like UCB1 [3] and Thompson Sampling [37, 39]. These classical methods assume stationary reward distributions, which are violated in our setting. Contextual bandits [9, 30] like LinUCB require all relevant features to be observable. Recent work on bandits with unobserved confounders [6, 15, 31] typically assumes access to instrumental variables or structural knowledge unavailable here.

Doubly-robust approaches. While intended to reduce bias, doubly-robust approaches [12, 23] also sever feedback-induced confounding ($s_{t-1} \rightarrow r_{t-1} \rightarrow a_t$ and $s_{t-1} \rightarrow s_t \rightarrow r_t$ in Figure 1). However, they often introduce high variance through inverse propensity weights and estimate rewards averaged over a state distribution rather than adapting to the current hidden state.

Non-stationary and adversarial bandit. Non-stationary algorithms use sliding windows or discounting [8, 10, 16] to treat changes as arbitrary drift. Semiparametric variants [25] allow non-stationarity but lack the flexibility to handle shifts in arm rankings or gaps. Adversarial algorithms like EXP3 [4] target the single retrospective best arm, which leads to overly conservative exploration when aiming for dynamic regret. We focus instead on a structured Markovian state determining the reward mapping.

Restless bandit and reinforcement learning. Restless bandits [32, 41] model Markovian dynamics, but assume observable states and known, action-dependent transitions. In reinforcement learning, Partially observable MDPs (POMDPs) [22, 34] assume decodability [5, 14, 21, 42] to distinguish hidden states, which does not hold here. Furthermore, POMDP transitions are action-dependent, whereas our state evolution is autonomous. Contextual bandits in Markov

environments [17, 33] or information-theoretic approaches [2, 18] similarly require full observability or sufficient statistics.

Latent Markov decision processes. Highly relevant is work on Latent Markov decision processes (LMDPs) [26–28]. However, LMDPs assume an episodic structure with contexts fixed throughout an episode. Our setting considers continuous online learning in a single interaction sequence without episodes. Our model-free approach avoids the computational burden of learning reward distributions, facilitating deployment in large-scale applications like online advertising.

We summarize these differences in Table 4.

2 Setup and Notations

Latent-state bandit model. We consider a non-stationary multi-armed bandit problem with K arms, S hidden states, and a time horizon of T rounds. At each round $t = 1, 2, \dots, T$, the environment occupies a hidden state $s_t = 1, 2, \dots, S$ that is unobservable to the agent. The hidden state evolves according to a Markov chain with transition matrix \mathbf{P} , where $P_{ij} = \mathbb{P}(s_{t+1} = j \mid s_t = i)$ denotes the probability of transitioning from state i to state j . We assume the chain is ergodic with stationary distribution π^* .

Upon selecting an arm $a_t = 0, \dots, K - 1$, the agent observes a stochastic reward

$$r_t = \mu_{s_t, a_t} + \eta_t,$$

where $\mu_{s, a} \in [0, 1]$ is the mean reward of arm a in state s and η_t is mean zero with variance σ^2 . The agent never observes the state s_t directly — only the scalar reward r_t .

Dynamic regret. For each state s , define an optimal arm $a_s^* \in \arg \max_{a \in \mathcal{A}} \mu_{s, a}$ and gaps $\Delta_{s, a} := \mu_{s, a^*} - \mu_{s, a} \geq 0$. Let $\Delta_{\max} := \max_{s \in \mathcal{S}, a \in \mathcal{A}} \Delta_{s, a} \leq 1$ denote the maximum single-step regret. The (single-unit) dynamic regret against the state-aware oracle is

$$R_T := \sum_{t=1}^T \Delta_{s_t, a_t}.$$

Notations. Our algorithms construct context features from past observations to enable state inference. We write $\phi_t \in \mathbb{R}^d$ for the context vector at round t , where the specific construction depends on the algorithm. For LC-UCB, we could use the lagged context $\phi_t = (a_{t-1}, r_{t-1})$, concatenating the previous action¹ with the previous reward. For probing algorithms (RP-UCB and its variants), we additionally incorporate joint observations $(r_0^{\text{prev}}, r_1^{\text{prev}})$ obtained by sampling both arms.

All algorithms build upon the LinUCB algorithm [30]. For each arm a , we maintain a precision matrix $\mathbf{A}_a \in \mathbb{R}^{d \times d}$, a reward-weighted feature vector $\mathbf{b}_a \in \mathbb{R}^d$, and compute parameter estimates $\hat{\theta}_a = \mathbf{A}_a^{-1} \mathbf{b}_a$. Arm selection follows the upper confidence bound principle: at each round, we select $a_t = \arg \max_a \text{UCB}_{t, a}$, where $\text{UCB}_{t, a} = \phi_t^\top \hat{\theta}_a + \alpha \sqrt{\phi_t^\top \mathbf{A}_a^{-1} \phi_t}$ and $\alpha > 0$ controls exploration. The regularization parameter $\lambda > 0$ initializes the precision matrices as $\mathbf{A}_a = \lambda \mathbf{I}$.

For fixed-schedule probing, the parameter τ specifies the probing frequency. For adaptive probing, we use thresholds z_{thresh} (residual gate), m_{thresh} (uncertainty gate), and (λ_h, δ_h) (hazard gate), along

¹or, where appropriate, a one-hot encoding thereof to apply LinUCB

with a minimum inter-probe gap τ_{\min} . Table 1 summarizes the key symbols for reference.

Symbol	Description
K	Number of arms
S	Number of hidden states
T	Time horizon
s_t	Hidden state at round t
a_t	Arm selected at round t
r_t	Reward at round t
$\mu_{s, a}$	Expected reward (arm a , state s)
\mathbf{P}	State transition matrix
ϕ_t	Context vector at round t
\mathbf{A}_a	Precision matrix for arm a
$\hat{\theta}_a$	Parameter estimate for arm a
$\text{UCB}_{t, a}$	Upper confidence bound
α	Exploration parameter
λ	Regularization parameter
τ	Probing frequency
τ_{\min}	Minimum inter-probe gap

Table 1: Summary of key notation.

3 Lagged Action-Reward as Context

The main challenge in our setting is that reward distributions depend on hidden states that evolve over time. Since direct state observation is impossible, we must develop algorithms that infer state information indirectly from observable quantities. This section introduces LC-UCB in Algorithm 1, which utilizes a simple but powerful insight: under Markovian state dynamics, recent rewards carry information about the current hidden state.

Consider the information available to the agent at time t . While the current state s_t is unobservable, the agent has access to the previous action a_{t-1} and the resulting reward r_{t-1} . Since the reward r_{t-1} was generated from a conditional distribution fully determined by a_{t-1} and s_{t-1} , the previous action-reward pair (a_{t-1}, r_{t-1}) provides information about s_{t-1} . If the hidden state evolves as a Markov chain slowly and the mixing time is long, the previous state s_{t-1} is highly informative of the current state s_t . Therefore, the previous action-reward pair (a_{t-1}, r_{t-1}) acts as an informative proxy about the current state s_t , and we can use the pair as a contextual feature and applying contextual bandit algorithms to learn state-dependent reward mappings.

3.1 Intuition

We provide a bit more intuition on why one may expect LC-UCB to perform better than their standard algorithm counterpart such as UCB1.

What UCB1 Estimates. UCB1 maintains empirical means

$$\hat{\mu}_{t, a} = \frac{1}{N_{t, a}} \sum_{i=1}^t r_i \mathbf{1}_{a_i=a}, \quad \text{where } N_{t, a} = \#\{i : 1 \leq i \leq t \text{ and } a_i = a\},$$

for each arm a , which simply neglects the existence of an evolving state s_t . Since the hidden state Markov chain is ergodic, the state

Algorithm 1: Lagged-Context Upper Confidence Bound (LC-UCB)

Data: $\alpha > 0$ (exploration parameter), $\lambda > 0$ (regularization), T (time horizon), K (number of arms)

- 1 **for** $a \leftarrow 0, 1, \dots, K-1$ **do**
- 2 Initialize LinUCB model \mathcal{M}_a with exploration parameter α and regularization λ ;
- 3 $(a_0, r_0) \leftarrow (0, 0)$; // Initialize previous action and reward
- 4 **for** $t \leftarrow 1, 2, \dots, T$ **do**
- 5 $\phi_t \leftarrow (a_{t-1}, r_{t-1})$;
- 6 **for** $a \leftarrow 0, 1, \dots, K-1$ **do**
- 7 Compute $UCB_{t,a}$ using LinUCB model \mathcal{M}_a with context ϕ_t ;
- 8 $a_t \leftarrow \arg \max_a UCB_{t,a}$; // Select arm
- 9 Play action a_t and observe reward r_t ;
- 10 Update LinUCB model \mathcal{M}_{a_t} with (ϕ_t, r_t) ;

visiting distribution converges to some π_{UCB}^* . So as $t \rightarrow \infty$, the empirical means $\hat{\mu}_{a,t}$ should converge to $\mathbb{E}_{a \sim \pi_{UCB}^*(s)} \mu_{s,a}$ and UCB1 effectively solves

$$a^{UCB1} = \arg \max_a \mathbb{E}_{a \sim \pi_{UCB}^*(s)} \mu_{s,a}.$$

This finds the optimal arm under a certain state distribution, which may be suboptimal in individual states.

What LC-UCB Estimates. For each arm a , LC-UCB collects data

$$\mathcal{D}_a = \{(a_{t-1}, r_{t-1}, r_t) : a_t = a\}.$$

The algorithm proceeds to learn a mapping from the context (a_{t-1}, r_{t-1}) to r_t . Now

$$\begin{aligned} \mathbb{E}[r_t \mid a_{t-1} = a', r_{t-1} = r'] \\ = \sum_s \mathbb{P}[s_t = s \mid a_{t-1} = a', r_{t-1} = r'] \cdot \mu_{s,a}. \end{aligned} \quad (1)$$

For a Markov chain with slow mixing time, we would expect

$$\mathbb{P}[s_t = s \mid a_{t-1} = a', r_{t-1} = r'] \approx \mathbb{P}[s_{t-1} = s \mid a_{t-1} = a', r_{t-1} = r'].$$

Now by Bayes rule, we have

$$\begin{aligned} \mathbb{P}[s_{t-1} = s \mid a_{t-1} = a', r_{t-1} = r'] \\ \propto \pi_{LC-UCB}^*(s, a') \cdot \mathbb{P}[r_{t-1} = r' \mid s_{t-1} = s, a_{t-1} = a'] \end{aligned}$$

where $\pi_{LC-UCB}^*(s', a')$ is the algorithm-dependent probability that each pair (s', a') is visited.

If the rewards are well-separated, then we should expect s to maximize $\mathbb{P}[r_{t-1} = r' \mid s_{t-1} = s, a_{t-1} = a']$; and if $\pi_{LC-UCB}^*(s', a')$ is “well-behaved”, then we should also expect s to maximize $\mathbb{P}[s_t = s \mid a_{t-1} = a', r_{t-1} = r']$. Now it follows from (1) that

$$\mathbb{E}[r_t \mid a_{t-1} = a', r_{t-1} = r'] \approx \mu_{s,a}.$$

In other words, this conditional expectation well-approximates the expected reward that we get at the true s_{t-1} . Given that this expected reward is well-estimated for all a , LC-UCB then proceed to pick one that maximizes $\mu_{s,a}$.

One potential issue that may arise is that there may exist multiple u 's such that $\mathbb{P}[r_{t-1} = r' \mid s_{t-1} = s, a_{t-1} = a']$ is non-negligible. In other words, given the reward information r_{t-1} , there are multiple possible values of the unobserved state s . If one misspecifies the s , then maximizing over all arm a would lead to the wrong policy. This motivates the probing scheme that we introduce later.

4 Probing for State Fingerprint

While LC-UCB demonstrates strong performance in many scenarios, this approach has a fundamental limitation: when multiple states produce similar rewards for the same arm, the lagged context cannot distinguish between them². This section introduces probing strategies that resolve state ambiguity by constructing richer observations we call *state fingerprints*.

Example 1. Consider the illustrative example shown in Table 2, where each entry is the mean reward under the given state and arm. When LC-UCB observes the context $(a_{t-1} = 0, r_{t-1} = 0.4)$, this observation is consistent with two possible states: states 0 and 1. Critically, these states have different optimal arms: arm 0 is optimal in state 0 (since $0.4 > 0.3$), while arm 1 is optimal in state 1 (since $0.5 > 0.4$). Thus, the lagged context alone can be non-identifying in such scenarios, motivating a probing approach.

	State 0	State 1	State 2	State 3
Arm 0	0.4	0.4	0.6	0.6
Arm 1	0.3	0.5	0.5	0.3
Fingerprint (r_0, r_1)	(0.4, 0.3)	(0.4, 0.5)	(0.6, 0.5)	(0.6, 0.3)

Table 2: Reward Matrix in Example 1.

This ambiguity is not merely a pathological edge case. As the number of states S increases, the chance of having reward overlap across states grows substantially. This creates widespread ambiguity where single-arm observations become uninformative about the optimal arm corresponding to the underlying state. This suggests that the performance of LC-UCB may degrade significantly in environments with a large state space and complex reward patterns.

The solution is to observe rewards from multiple arms in the same state. Consider what happens if we sample both arms: Each state now has a unique fingerprint – a pair of rewards that jointly identify the state even when individual rewards do not. In Table 2, states 0 and 1, previously indistinguishable, are now separated: (0.4, 0.3) vs (0.4, 0.5).

This insight connects to the principle of randomized controlled experiments [24, 36]: by simultaneously exposing different experimental units to different treatments, we can directly compare outcomes and resolve confounding from unobserved variables. In the bandit setting, this translates to deliberately assigning different arms to different decision units, allowing the algorithm to observe joint reward realizations (r_0, r_1) that provide disambiguating information about the underlying state.

²Similar to the statistical notion of identifiability

4.1 Two Probing Paradigms

We develop two algorithms based on how fingerprints are collected, presented in Algorithms 2 and 3. We implemented for a two arms, but believe that it can be easily generalized to multiple arms.

- (1) Randomized Probing UCB (RP-UCB): Some applications naturally support simultaneous experimentation: online platforms can randomize different users to different recommendation algorithms [1, 38], clinical trials can assign different patients to different treatment protocols [7, 29, 40], and financial trading systems can allocate portions capital to different strategies [19]. In these settings, we can obtain true joint observations (r_0, r_1) from the same time period.
- (2) Sequential Probing UCB (SP-UCB): When only a single decision-making unit exists, simultaneous probing is impossible. Instead, we sample arms consecutively — playing arm 0 at time t , then arm 1 at time $t+1$, and treat (r_t, r_{t+1}) as a synthetic fingerprint. This approach relies on slow state transitions: if the hidden state is sufficiently “sticky” (i.e., with high self-transition probability), consecutive observations approximate true joint observations.

4.2 Feature Construction

Both algorithms combine fingerprint information with lagged context to form the feature vector

$$\phi_t := \phi_{\text{fp}} \oplus \phi_{\text{lag}} = (r_0^{\text{fp}}, r_1^{\text{fp}}) \oplus (a_{t-1}, r_{t-1}) \quad (2)$$

where \oplus denotes vector concatenation. The two components are defined as:

- (1) Fingerprint features: $\phi_{\text{fp}} := (r_0^{\text{fp}}, r_1^{\text{fp}})$ captures the most recent joint observation from probing.
- (2) Lagged features: $\phi_{\text{lag}} := (a_{t-1}, r_{t-1})$ captures the previous action³ a_{t-1} and the previous reward r_{t-1} .

Fingerprints provide long-term state disambiguation but are collected infrequently (at a fixed interval of every τ rounds). Between probes, the fingerprint features remain constant, potentially becoming stale if the hidden state transitions. Lagged context compensates by providing continuous short-term state tracking: even when the fingerprint is outdated, the previous reward r_{t-1} reflects the most recent state information. The combination leverages both timescales — fingerprints anchor the state estimate, while lagged context refines it with up-to-date observations.

Intuitively, the probing interval trades off a fixed regret incurred by probing, and the regret from stale state information, as demonstrated in Theorem 1.

Theorem 1. Suppose $S = 2$ and each state has a unique optimal arm. Suppose further that the Markov chain satisfies $\mathbb{P}(s_{t+1} \neq s_t) \leq q$ for all t . Consider an idealized periodic probing policy that probes once every τ rounds. Each probe incurs regret at most Δ_{probe} and returns an estimate of the current optimal arm with error probability at most ε_{fp} . Between probes, the policy exploits by repeatedly playing the estimated optimal arm. Then

$$\frac{1}{T} \mathbb{E}[R_T] \leq \frac{\Delta_{\text{probe}}}{\tau} + \frac{\Delta_{\text{max}} q \tau}{2} + \Delta_{\text{max}} \varepsilon_{\text{fp}} + O\left(\frac{1}{T}\right).$$

³or, where appropriate, a one-hot coding thereof

Algorithm 2: Randomized Probing Upper Confidence Bound (RP-UCB)

```

Data:  $\alpha, \lambda, \tau$  (probing interval),  $T, K \leftarrow 2$ 
1 for  $a \leftarrow 0, 1$  do
2   Initialize LinUCB model  $\mathcal{M}_a$  with exploration parameter
    $\alpha$  and regularization  $\lambda$ 
3    $(r_0^{\text{fp}}, r_1^{\text{fp}}) \leftarrow (0, 0)$ ; // Initialize fingerprint
4    $(a_0, r_0) \leftarrow (0, 0)$ ; // Init. prev. action and reward
5   for  $t \leftarrow 1, 2, \dots, T$  do
6      $\phi_{\text{fp}} \leftarrow (r_0^{\text{fp}}, r_1^{\text{fp}})$ ; // Fingerprint features
7      $\phi_{\text{lag}} \leftarrow (a_{t-1}, r_{t-1})$ ; // Lagged features
8      $\phi_t \leftarrow \phi_{\text{fp}} \oplus \phi_{\text{lag}}$ ;
9     if  $t \bmod \tau = 0$  then
10      mode  $\leftarrow$  probe; // Probe mode
11       $(a_t^C, a_t^T) \leftarrow (0, 1)$ ;
12    else
13      mode  $\leftarrow$  exploit; // Exploit mode
14      for  $a \leftarrow 0, 1$  do
15        Compute  $\text{UCB}_{t,a}$  using LinUCB model  $\mathcal{M}_a$  with
        context  $\phi_t$ ;
16         $a^* \leftarrow \arg \max_a \text{UCB}_{t,a}$ ;
17         $(a_t^C, a_t^T) \leftarrow (a^*, a^*)$ ;
18      Play actions  $(a_t^C, a_t^T)$  and observe rewards  $(r_t^C, r_t^T)$ ;
19      Update LinUCB models  $\mathcal{M}_{a_t^C}$  and  $\mathcal{M}_{a_t^T}$  with  $(\phi_t, r_t^C)$ 
      and  $(\phi_t, r_t^T)$ ;
20      if mode = probe then
21         $(r_0^{\text{fp}}, r_1^{\text{fp}}) \leftarrow (r_t^C, r_t^T)$ ;
22        if  $r_t^T > r_t^C$  then
23           $(a_t, r_t) \leftarrow (a_t^T, r_t^T)$ ;
24        else
25           $(a_t, r_t) \leftarrow (a_t^C, r_t^C)$ ;
26      else
27         $(a_t, r_t) \leftarrow (a_t^C, (r_t^C + r_t^T)/2)$ ;

```

Ignoring ε_{fp} , the bound is minimized at $\tau^ \asymp \sqrt{\Delta_{\text{probe}}/(\Delta_{\text{max}} q)}$.*

PROOF SKETCH. The probe cost contributes at most Δ_{probe} every τ rounds. Between probes, regret occurs when the state has changed since the last probe (stale fingerprint) or when the probe misidentifies the optimal arm. A union bound gives $\mathbb{P}(s_{t_0+j} \neq s_{t_0}) \leq jq$ within a length- τ interval, and summing $j = 1, \dots, \tau - 1$ yields the stated staleness term. A probe misclassification leads to at most Δ_{max} regret per round until the next probe, hence contributes $\Delta_{\text{max}} \varepsilon_{\text{fp}}$ on average. \square

5 Upper Confidence Bound with Adaptive Probing

While probing strategies like RP-UCB and SP-UCB provide a principled approach to information gathering, every probing incurs a cost for playing suboptimal arms. The fixed probing schedule creates a fundamental inefficiency: the algorithm pays the same

Algorithm 3: Sequential Probing Upper Confidence Bound (SP-UCB)

```

Data:  $\alpha, \lambda, \tau, T, K \leftarrow 2$ 
// (Omitted) Lines 1-4 from Algorithm 2
1 for  $t \leftarrow 1, 2, \dots, T$  do
    // (Omitted) Lines 6-8 from Algorithm 2
    2 if  $t \bmod \tau \in \{0, 1\}$  then
        mode  $\leftarrow$  probe; // Probe mode
        3  $a_t \leftarrow t \bmod \tau$ ;
    5 else
        mode  $\leftarrow$  exploit; // Exploit mode
        7 for  $a \leftarrow 0, 1$  do
            8 Compute  $UCB_{t,a}$  using LinUCB model  $\mathcal{M}_a$  with
            context  $\phi_t$ ;
            9  $a_t \leftarrow \arg \max_a UCB_{t,a}$ ;
    10 Play action  $a_t$  and observe reward  $r_t$ ;
    11 if mode = probe and  $a_t = 1$  then
        12  $(r_0^{\text{fp}}, r_1^{\text{fp}}) \leftarrow (r_{t-1}, r_t)$ ;
    13 Update  $\mathcal{M}_{a_t}$  with  $(\phi_t, r_t)$ ;

```

probing cost regardless of its evolving information needs. Early in learning, when the model is uncertain, frequent probing accelerates convergence. Later, when the model is confident, excessive probing wastes exploitation opportunities. Similarly, if prediction errors suddenly spike, which suggests state drift or model inadequacy, immediate probing would be valuable regardless of the schedule.

To overcome these shortcomings, we introduce adaptive probing where the decision to probe is governed by data-driven criteria rather than a fixed schedule. The adaptive probing variant of RP-UCB (Algorithm 2) is AdaRP-UCB and presented in Algorithm 4, and the analogous variant of SP-UCB (Algorithm 3) is AdaSP-UCB and shown in Algorithm 5 in the appendix.

5.1 Adaptive Gating Mechanism

We propose three complementary gates that collectively assess whether probing is warranted. Each gate monitors a different signal, and probing is triggered when any gate activates, subject to a minimum gap constraint.

- Residual gate detects model drift. The residual gate monitors prediction errors. If the model accurately captures the state-reward relationship, residuals should be small. Large residuals indicate either model misspecification or a state transition that invalidates the current fingerprint. At each round, we compute the Studentized residual

$$z_{t-1} = \frac{r_{t-1} - \hat{r}_{t-1}}{\sqrt{\text{Var}(\hat{r}_{t-1}) + \sigma_0^2}}$$

where $\hat{r}_{t-1} = \phi_{t-1}^\top \hat{\theta}_{a_{t-1}}$ is the predicted reward, $\text{Var}(\hat{r}_{t-1}) = \phi_{t-1}^\top \mathbf{A}_{a_{t-1}}^{-1} \phi_{t-1}$ is the model uncertainty, and σ_0^2 is ideally the observation noise variance σ^2 , but serves primarily as a floor to prevent the residual gate from triggering too often.

The residual gate activates when the absolute residual exceeds a threshold.

$$g_{\text{res}} := \mathbf{1} [|z_{t-1}| \geq z_{\text{thresh}}].$$

Under correct model specification and no state transition, z_{t-1} is approximately standard normal. Setting $z_{\text{thresh}} \approx 2$ corresponds to probing when residuals fall outside a 95% confidence interval.

- Uncertainty gate resolves decision confidence. The uncertainty gate monitors the confidence gap between arms. When UCB scores are similar, the algorithm cannot reliably distinguish the optimal arm, and probing provides disambiguating information. We compute the UCB margin as $m_t = |UCB_{t,0} - UCB_{t,1}|$.

The uncertainty gate activates when the margin falls below a threshold.

$$g_{\text{unc}} := \mathbf{1} [m_t \leq m_{\text{thresh}}].$$

A small margin means the confidence intervals overlap substantially. Probing collects new fingerprint data that can sharpen the estimates and break the tie.

- Staleness gate prevents information stagnation. The staleness gate ensures that the algorithm eventually probes even when residuals are small and margins are large. This guards against scenarios where the model is confidently wrong due to outdated fingerprint information. We use an exponential hazard function based on time since last probe

$$h(t) = 1 - \exp(-\lambda_h(t - t_{\text{probe}})).$$

The staleness gate activates when the hazard exceeds a threshold.

$$g_{\text{haz}} := \mathbf{1} [h(t) \geq \delta_h].$$

The hazard $h(t)$ starts at 0 immediately after a probe and increases toward 1 over time. With $\lambda_h = 0.1$ and $\delta_h = 0.5$, the gate activates after approximately 7 rounds without probing. This provides a soft upper bound on the inter-probe interval.

Combining the three gates, the algorithm probes when any gate activates, subject to a minimum gap.

$$\text{Probe at } t \iff (g_{\text{res}} \vee g_{\text{unc}} \vee g_{\text{haz}}) \wedge (t - t_{\text{probe}} \geq \tau_{\min}).$$

The minimum gap τ_{\min} prevents oscillatory behavior where the algorithm probes excessively in response to transient fluctuations.

6 Experiments

We conduct a comprehensive evaluation of our proposed adaptive probing algorithms against established baselines.⁴ Our test environment consists of a two-armed bandit with S hidden states, where each state-arm pair has normally distributed rewards $\mathcal{N}(\mu_{s,a}, \sigma^2)$ and states evolve according to a Markov chain with high self-transition probability p_{stay} . We compare our algorithms against both classical bandit methods (UCB1, Thompson Sampling, EXP3) and popular non-stationary bandit algorithms (Sliding Window UCB, Discounted UCB, EXP3-S). Note that these algorithms fall into two distinct categories: *randomization algorithms* (AdaRP-UCB

⁴Please refer to Table 5 for quick reference of all algorithms that we consider, and our implementation of these algorithms and their evaluation can be accessed at <https://github.com/xxx/xxx>.

Algorithm 4: Adaptive Randomized Probing Upper Confidence Bound (AdaRP-UCB)

Data: $\alpha, \lambda, z_{\text{thresh}}, \sigma_0, m_{\text{thresh}}, \lambda_h, \delta_h, \tau_{\min}, T$

- 1 **for** $a \leftarrow 0, 1$ **do**
- 2 Initialize LinUCB model \mathcal{M}_a with exploration parameter α and regularization λ
- 3 $(r_0^{\text{fp}}, r_1^{\text{fp}}) \leftarrow (0, 0)$; // Initialize fingerprint
- 4 $(a_0, r_0) \leftarrow (0, 0)$; // Init. prev. action and reward
- 5 $t_{\text{probe}} \leftarrow 0$;
- 6 **for** $t = 1, 2, \dots, T$ **do**
- 7 $\phi_{\text{fp}} \leftarrow (r_0^{\text{fp}}, r_1^{\text{fp}})$; // Fingerprint features
- 8 $\phi_{\text{lag}} \leftarrow (a_{t-1}, r_{t-1})$; // Lagged features
- 9 $\phi_t \leftarrow \phi_{\text{fp}} \oplus \phi_{\text{lag}}$;
- 10 **for** $a \leftarrow 0, 1$ **do**
- 11 Compute $\text{UCB}_{t,a}$ using LinUCB model \mathcal{M}_a with context ϕ_t ;
- 12 $g \leftarrow \text{ComputeGates}$;
- 13 **if** g **then**
- 14 mode $\leftarrow \text{probe}$; // Probe mode
- 15 $(a_t^C, a_t^T) \leftarrow (0, 1)$;
- 16 $t_{\text{probe}} \leftarrow t$;
- 17 **else**
- 18 mode $\leftarrow \text{exploit}$; // Exploit mode
- 19 $a^* \leftarrow \arg \max_a \text{UCB}_{t,a}$;
- 20 $(a_t^C, a_t^T) \leftarrow (a^*, a^*)$;
- 21 Play actions (a_t^C, a_t^T) and observe reward (r_t^C, r_t^T) ;
- 22 Update LinUCB models $\mathcal{M}_{a_t^C}$ and $\mathcal{M}_{a_t^T}$ with (ϕ_t, r_t^C) and (ϕ_t, r_t^T) ;
- 23 **if** mode $= \text{probe}$ **then**
- 24 $(r_0^{\text{fp}}, r_1^{\text{fp}}) \leftarrow (r_t^C, r_t^T)$;
- 25 **if** $r_t^T > r_t^C$ **then**
- 26 $(a_t, r_t) \leftarrow (a_t^T, r_t^T)$;
- 27 **else**
- 28 $(a_t, r_t) \leftarrow (a_t^C, r_t^C)$;
- 29 **else**
- 30 $(a_t, r_t) \leftarrow (a_t^C, (r_t^C + r_t^T)/2)$;
- 31 **Function** *ComputeGates*:
- 32 // Residual gate
- 33 $\hat{r}_{t-1} \leftarrow \phi_{t-1}^T \hat{\theta}_{a_{t-1}}$;
- 34 $v_{t-1} \leftarrow \phi_{t-1}^T A_{a_{t-1}}^{-1} \phi_{t-1}$;
- 35 $z_{t-1} \leftarrow \frac{r_{t-1} - \hat{r}_{t-1}}{\sqrt{v_{t-1} + \sigma_0^2}}$;
- 36 $g_{\text{res}} = \mathbf{1}[|z_{t-1}| \geq z_{\text{thresh}}]$;
- 37 // Uncertainty gate
- 38 $m_t = |\text{UCB}_{t,0} - \text{UCB}_{t,1}|$;
- 39 $g_{\text{unc}} = \mathbf{1}[m_t \leq m_{\text{thresh}}]$;
- 40 // Staleness gate
- 41 $g_{\text{haz}} = \mathbf{1}[1 - \exp(-\lambda_h(t - t_{\text{probe}})) \geq \delta_h]$;
- 42 **return** $(g_{\text{res}} \vee g_{\text{unc}} \vee g_{\text{haz}}) \wedge (t - t_{\text{probe}} \geq \tau_{\min})$;

Algorithm 5: Adaptive Sequential Probing Upper Confidence Bound (AdaSP-UCB)

Data: $\alpha, \lambda, z_{\text{thresh}}, \sigma_0, m_{\text{thresh}}, \lambda_h, \delta_h, \tau_{\min}, T$
 // (Omitted) Lines 1-5 from Algorithm 4

- 1 mode $\leftarrow \text{exploit}$;
- 2 **for** $t = 1, 2, \dots, T$ **do**
- 3 // (Omitted) Lines 7-12 from Algorithm 4
- 4 **if** mode $= \text{exploit}$ **then**
- 5 **if** g **then**
- 6 mode $\leftarrow \text{probe}$; // Probe mode
- 7 probe_arm $\leftarrow 0$; // Start probing arm 0
- 8 **if** mode $= \text{probe}$ **then**
- 9 $a_t \leftarrow \text{probe_arm}$;
- 10 probe_arm $\leftarrow \text{probe_arm} + 1$; // Probe the next arm next time
- 11 **else**
- 12 $a_t \leftarrow \arg \max_a \text{UCB}_{t,a}$;
- 13 Play action a_t and observe reward r_t ;
- 14 **if** mode $= \text{probe}$ and probe_arm $= 2$ **then**
- 15 mode $\leftarrow \text{exploit}$; // Completed sequential probing
- 16 $(r_0^{\text{fp}}, r_1^{\text{fp}}) \leftarrow (r_{t-1}, r_t)$;
- 17 Update \mathcal{M}_{a_t} with (ϕ_t, r_t) ;

and RP-UCB) that simultaneously manage two units during the learning process, and *single-unit algorithms* that operate with a unified decision unit. We double the noise variance for randomized algorithms to compensate for their inherent randomization effects and ensure fair comparison.

We systematically vary four key environmental parameters: the number of states $S \in \{2, 10, 20, 50\}$, the persistence parameter $p_{\text{stay}} \in \{0.5, 0.8, 0.9, 0.95, 0.99\}$, the reward noise standard deviation $\sigma \in \{0.01, 0.05, 0.1, 0.5\}$, and the time horizon $T \in \{500, 1000, 5000, 20000\}$. For each parameter configuration, we generate 128 random problem instances with uniformly sampled reward means $\mu_{s,a} \sim \text{Uniform}[0, 1]$, and evaluate each algorithm over 5 independent runs per instance. Our evaluation metrics include cumulative regret (sum of instantaneous regrets over all rounds) and winning rates (the fraction of instances where each algorithm achieves the lowest regret).

The mean cumulative regrets are presented in Table 3. Among the randomization approaches, AdaRP-UCB demonstrates superior performance in 12 out of 13 experimental configurations, significantly outperforming RP-UCB particularly in volatile environments where its adaptive probing mechanisms excel at rapid context switching.

For single-unit algorithms, we observe a clear performance hierarchy: contextual methods (LC-UCB, LC-TS) and probing variants (AdaSP-UCB, SP-UCB) consistently outperform classical and non-stationary algorithms. In particular, AdaSP-UCB dominates under low reward noise, slow mixing and/or large state space, while contextual approaches perform the best for faster mixing. The only exception is that when reward noise is extremely high, e.g., $\sigma = 0.5$

Value	Varying Param.	Randomization				Single-Unit							Oracle	
		AdaRP-UCB	RP-UCB	AdaSP-UCB	D-UCB	EXP3	EXP3-S	LC-TS	LC-UCB	SP-UCB	SW-UCB	TS	UCB1	Opt. Single Arm
	Default	452.22	943.64	707.69	1553.94	4516.35	3452.92	1299.25	1530.02	1137.14	1476.74	5037.26	2763.03	4451.31
2	Number of States	342.58	933.81	585.72	1400.98	2366.72	2971.22	153.48	118.35	327.74	1393.97	2586.57	1102.10	2074.36
20	Number of States	467.12	948.49	712.65	1564.25	5149.11	3536.75	1450.52	1914.41	1244.48	1484.23	5681.02	3167.98	5192.14
50	Number of States	468.95	966.04	709.16	1585.24	5737.84	3623.26	1552.16	2066.59	1292.20	1500.65	6252.61	3504.34	5840.72
0.50	Self-transition Prob.	4007.60	4630.15	4516.70	4377.77	4751.64	5509.11	3659.89	3624.84	3739.32	4952.51	5323.92	4377.71	4572.14
0.80	Self-transition Prob.	2368.62	3412.53	2964.17	2995.52	4637.48	5326.39	2351.42	2407.24	2554.18	4039.61	5237.72	3487.36	4445.60
0.90	Self-transition Prob.	1600.62	2510.65	2153.95	2567.11	4706.50	5198.32	2031.90	2123.06	2259.17	3441.85	5395.82	3197.33	4541.32
0.95	Self-transition Prob.	1065.21	2017.19	1514.30	2209.35	4885.10	4977.90	1694.93	1783.73	1907.38	2807.29	5490.35	3064.73	4760.40
0.05	Reward Noise SD.	644.76	1075.98	814.56	1548.92	4589.35	3502.60	1225.25	1363.40	1127.96	1491.20	5287.53	2853.86	4573.26
0.10	Reward Noise SD.	1330.41	1379.29	1444.04	1541.61	4558.92	3458.40	1157.71	1254.24	1202.42	1507.11	5267.70	2783.66	4491.77
0.50	Reward Noise SD.	3960.63	3872.88	4118.41	1870.63	4637.03	3573.40	2842.84	2480.63	2840.06	2041.06	5741.33	3119.61	4544.59
500	Number of Rounds	16.01	24.69	23.85	37.32	98.90	90.01	36.37	23.20	23.38	36.78	95.03	44.90	117.45
1000	Number of Rounds	30.22	48.74	45.40	72.79	207.13	178.43	70.23	53.38	48.18	72.54	215.67	99.92	233.18
5000	Number of Rounds	125.89	242.22	192.60	385.43	1131.87	872.31	341.68	364.29	285.26	371.11	1286.11	612.66	1135.05

Table 3: Cumulative regret for Various Parameters and Algorithms

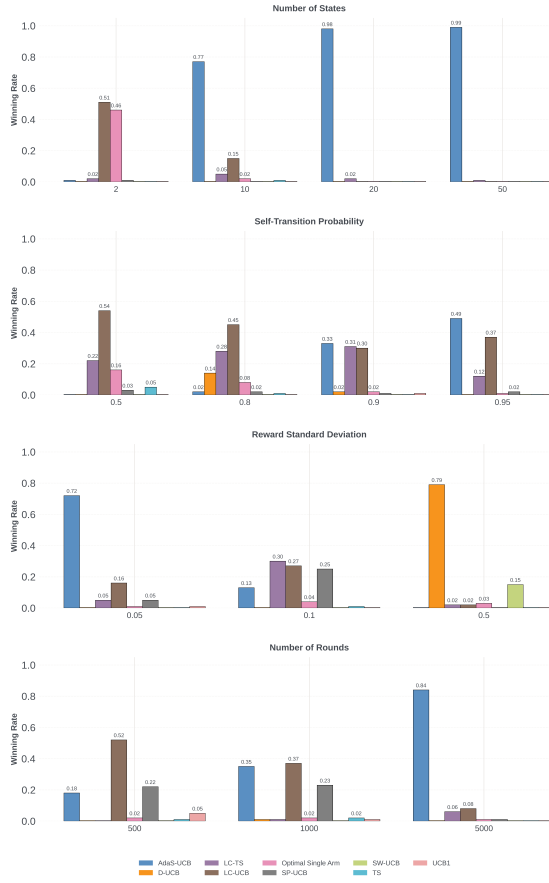


Figure 2: Head-to-head winning rates under different problem-specific parameters.

while for each arm the expected mean reward gap is ≈ 0.1 , our algorithms underperform D-UCB and SW-UCB. In these settings, the state fingerprints are less informative about the state, so probing may be triggered often with little benefits in return. The winning rate analysis, as shown in Figure 2, provide additional insights into the relative performance of the algorithms in different context.

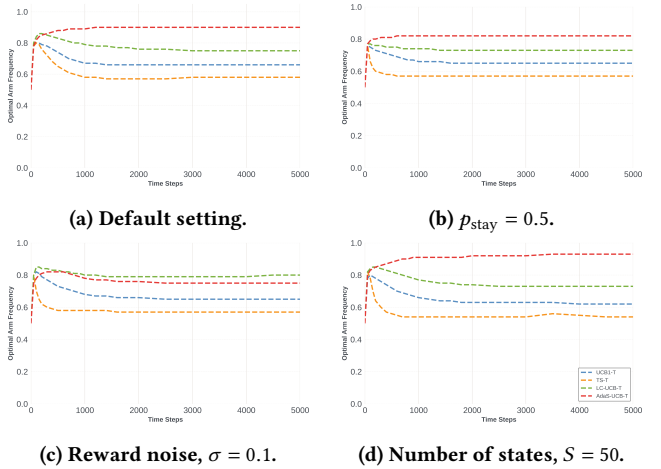


Figure 3: Frequency of pulling the optimal arm across time.

We also conduct an optimal arm frequency analysis, by measuring how often each algorithm selects the theoretically best arm $\{a_t^*\}_{t=1}^T$ given the oracle knowledge of the hidden state sequence $\{u_t\}_{t=1}^T$. This metric provides insights into algorithm adaptation capabilities. In Figure 3 we visualize the results for the default setting as well as three varying environmental parameters, with appropriate smoothing over a sliding window.

7 Conclusion

In this paper, we provided a setting where traditional contextual bandit algorithms cannot achieve zero average regret with respect to the dynamically optimal policy, as the action-reward mapping is confounded by unobserved Markovian state. We propose a family of algorithms that utilizes the immediate action-reward pair and strategically probed reward observations. A combination of these allowed us to obtain incomplete information about the hidden state, and contributes to a lower, albeit, nonzero average regret. We demonstrated the capability of this approach in our simulations, while highlighting the best choice of algorithm in various settings, e.g., varying number of states, varying self-transition probabilities, varying noise level of the reward.

Outside of the degenerative scenario where we have perfect information about the underlying state, we believe that zero regret cannot be achieved. Future work includes characterizing alternative types of regret. Furthermore, all past action-reward pairs provide some information about the current state. Taking this premise to its logical conclusion, we may wish to supply the entire sequence of past action-reward pairs, which is impractical. More adaptation should be possible to balance better information about the state and the curse of dimensionality.

References

- [1] Deepak Agarwal, Bee-Chung Chen, and Pradheep Elango. 2009. Explore/exploit schemes for web content optimization. In *2009 Ninth IEEE International Conference on Data Mining*. IEEE, 1–10.
- [2] Dilip Arumugam and Benjamin Van Roy. 2022. Deciding what to model: Value-equivalent sampling for reinforcement learning. *Advances in neural information processing systems* 35 (2022), 9024–9044.
- [3] Peter Auer, Nicolo Cesa-Bianchi, and Paul Fischer. 2002. Finite-time analysis of the multiarmed bandit problem. *Machine learning* 47, 2 (2002), 235–256.
- [4] Peter Auer, Nicolo Cesa-Bianchi, Yoav Freund, and Robert E Schapire. 2002. The nonstochastic multiarmed bandit problem. *SIAM journal on computing* 32, 1 (2002), 48–77.
- [5] Kamyar Azizzadenesheli, Alessandro Lazaric, and Animashree Anandkumar. 2016. Reinforcement learning of pomdps using spectral methods. In *Conference on Learning Theory*. PMLR, 193–256.
- [6] Elias Bareinboim, Andrew Forney, and Judea Pearl. 2015. Bandits with unobserved confounders: a causal approach. In *Proceedings of the 29th International Conference on Neural Information Processing Systems - Volume 1* (Montreal, Canada) (NIPS'15). MIT Press, Cambridge, MA, USA, 1342–1350.
- [7] Donald A Berry. 2012. Adaptive clinical trials in oncology. *Nature reviews Clinical oncology* 9, 4 (2012), 199–207.
- [8] Omar Besbes, Yonatan Gur, and Assaf Zeevi. 2019. Optimal exploration-exploitation in a multi-armed bandit problem with non-stationary rewards. *Stochastic Systems* 9, 4 (2019), 319–337.
- [9] Alina Beygelzimer, John Langford, Lihong Li, Lev Reyzin, and Robert Schapire. 2011. Contextual bandit algorithms with supervised learning guarantees. In *Proceedings of the Fourteenth International Conference on Artificial Intelligence and Statistics*. JMLR Workshop and Conference Proceedings, 19–26.
- [10] Yang Cao, Zheng Wen, Branislav Kveton, and Yao Xie. 2019. Nearly optimal adaptive procedure with change detection for piecewise-stationary bandit. In *The 22nd International Conference on Artificial Intelligence and Statistics*. PMLR, 418–427.
- [11] Wei Chen, Yajun Wang, and Yang Yuan. 2013. Combinatorial Multi-Armed Bandit: General Framework and Applications. In *Proceedings of the 30th International Conference on Machine Learning (Proceedings of Machine Learning Research, Vol. 28)*, Sanjoy Dasgupta and David McAllester (Eds.). PMLR, Atlanta, Georgia, USA, 151–159, Issue 1. <https://proceedings.mlr.press/v28/chen13a.html>
- [12] Maria Dimakopoulou, Zhengyuan Zhou, Susan Athey, and Guido Imbens. 2019. Balanced linear contextual bandits. In *Proceedings of the Thirty-Third AAAI Conference on Artificial Intelligence and Thirty-First Innovative Applications of Artificial Intelligence Conference and Ninth AAAI Symposium on Educational Advances in Artificial Intelligence* (Honolulu, Hawaii, USA) (AAAI'19/IAAI'19/EEAAI'19). AAAI Press, Article 423, 9 pages. doi:10.1609/aaai.v33i01.33013445
- [13] Audrey Durand, Charis Achilleos, Demetris Iacovides, Katerina Strati, Georgios D. Mitsis, and Joelle Pineau. 2018. Contextual Bandits for Adapting Treatment in a Mouse Model of de Novo Carcinogenesis. In *Proceedings of the 3rd Machine Learning for Healthcare Conference (Proceedings of Machine Learning Research, Vol. 85)*, Finale Doshi-Velez, Jim Fackler, Ken Jung, David Kale, Rajesh Ranganath, Byron Wallace, and Jenna Wiens (Eds.). PMLR, 67–82. <https://proceedings.mlr.press/v85/durand18a.html>
- [14] Yonathan Efroni, Chi Jin, Akshay Krishnamurthy, and Sobhan Miryoosefi. 2022. Provable reinforcement learning with a short-term memory. In *International Conference on Machine Learning*. PMLR, 5832–5850.
- [15] Andrew Forney, Judea Pearl, and Elias Bareinboim. 2017. Counterfactual data-fusion for online reinforcement learners. In *International conference on machine learning*. PMLR, 1156–1164.
- [16] Aurélien Garivier and Eric Moulines. 2011. On upper-confidence bound policies for switching bandit problems. In *International conference on algorithmic learning theory*. Springer, 174–188.
- [17] Assaf Hallak, Dotan Di Castro, and Shie Mannor. 2015. Contextual Markov Decision Processes. arXiv:1502.02259 [stat.ML] <https://arxiv.org/abs/1502.02259>
- [18] Botao Hao and Tor Lattimore. 2022. Regret bounds for information-directed reinforcement learning. *Advances in neural information processing systems* 35 (2022), 28575–28587.
- [19] David P Helmbold, Robert E Schapire, Yoram Singer, and Manfred K Warmuth. 1998. On-line portfolio selection using multiplicative updates. *Mathematical Finance* 8, 4 (1998), 325–347.
- [20] Peter Henderson, Ben Chugg, Brandon Anderson, and Daniel E. Ho. 2022. Beyond Ads: Sequential Decision-Making Algorithms in Law and Public Policy. In *Proceedings of the 2022 Symposium on Computer Science and Law* (Washington DC, USA) (CSLAW '22). Association for Computing Machinery, New York, NY, USA, 87–100. doi:10.1145/3511265.3550439
- [21] Chi Jin, Sham Kakade, Akshay Krishnamurthy, and Qinghua Liu. 2020. Sample-efficient reinforcement learning of undercomplete pomdps. *Advances in Neural Information Processing Systems* 33 (2020), 18530–18539.
- [22] Leslie Pack Kaelbling, Michael L Littman, and Anthony R Cassandra. 1998. Planning and acting in partially observable stochastic domains. *Artificial intelligence* 101, 1-2 (1998), 99–134.
- [23] Wonyoung Kim, Gi-Soo Kim, and Myunghee Cho Paik. 2021. Doubly robust thompson sampling with linear payoffs. In *Proceedings of the 35th International Conference on Neural Information Processing Systems (NIPS '21)*. Curran Associates Inc., Red Hook, NY, USA, Article 1211, 11 pages.
- [24] Ron Kohavi, Roger Longbotham, Dan Sommerfield, and Randal M Henne. 2009. Controlled experiments on the web: survey and practical guide. *Data mining and knowledge discovery* 18, 1 (2009), 140–181.
- [25] Akshay Krishnamurthy, Zhiwei Steven Wu, and Vasilis Syrgkanis. 2018. Semi-parametric Contextual Bandits. In *Proceedings of the 35th International Conference on Machine Learning (Proceedings of Machine Learning Research, Vol. 80)*, Jennifer Dy and Andreas Krause (Eds.). PMLR, 2776–2785. <https://proceedings.mlr.press/v80/krishnamurthy18a.html>
- [26] Jeongyeol Kwon, Yonathan Efroni, Constantine Caramanis, and Shie Mannor. 2021. Reinforcement learning in reward-mixing mdps. *Advances in Neural Information Processing Systems* 34 (2021), 2253–2264.
- [27] Jeongyeol Kwon, Yonathan Efroni, Constantine Caramanis, and Shie Mannor. 2023. Reward-mixing mdps with few latent contexts are learnable. In *International Conference on Machine Learning*. PMLR, 18057–18082.
- [28] Jeongyeol Kwon, Shie Mannor, Constantine Caramanis, and Yonathan Efroni. 2024. RL in latent mdps is tractable: Online guarantees via off-policy evaluation. *Advances in Neural Information Processing Systems* 37 (2024), 82726–82756.
- [29] Zhe Leung Lai, Philip W Lavori, and Olivia Yueh-Wen Liao. 2014. Adaptive choice of patient subgroup for comparing two treatments. *Contemporary clinical trials* 39, 2 (2014), 191–200.
- [30] Lihong Li, Wei Chu, John Langford, and Robert E Schapire. 2010. A contextual-bandit approach to personalized news article recommendation. In *Proceedings of the 19th international conference on World wide web*, 661–670.
- [31] Luofeng Liao, Zuyue Fu, Zhuoran Yang, Yixin Wang, Dingli Ma, Mladen Kolar, and Zhaoran Wang. 2024. Instrumental variable value iteration for causal offline reinforcement learning. *Journal of Machine Learning Research* 25, 303 (2024), 1–56.
- [32] Keqin Liu and Qing Zhao. 2010. Indexability of restless bandit problems and optimality of whittle index for dynamic multichannel access. *IEEE Transactions on Information Theory* 56, 11 (2010), 5547–5567.
- [33] Aditya Modi, Nan Jiang, Satinder Singh, and Ambuj Tewari. 2018. Markov decision processes with continuous side information. In *Algorithmic learning theory*. PMLR, 597–618.
- [34] Joelle Pineau, Geoffrey Gordon, and Sebastian Thrun. 2006. Anytime point-based approximations for large POMDPs. *Journal of Artificial Intelligence Research* 27 (2006), 355–380.
- [35] Herbert Robbins. 1952. Some aspects of the sequential design of experiments. *Bull. Amer. Math. Soc.* 58, 5 (1952), 527 – 535.
- [36] Donald B Rubin. 1974. Estimating causal effects of treatments in randomized and nonrandomized studies. *Journal of educational Psychology* 66, 5 (1974), 688.
- [37] Daniel J Russo, Benjamin Van Roy, Abbas Kazerouni, Ian Osband, Zheng Wen, et al. 2018. A tutorial on thompson sampling. *Foundations and Trends® in Machine Learning* 11, 1 (2018), 1–96.
- [38] Liang Tang, Romer Rosales, Ajit Singh, and Deepak Agarwal. 2013. Automatic ad format selection via contextual bandits. In *Proceedings of the 22nd ACM international conference on Information & Knowledge Management*, 1587–1594.
- [39] William R Thompson. 1933. On the likelihood that one unknown probability exceeds another in view of the evidence of two samples. *Biometrika* 25, 3/4 (1933), 285–294.
- [40] Sofia S Villar, Jack Bowden, and James Wason. 2015. Multi-armed bandit models for the optimal design of clinical trials: benefits and challenges. *Statistical science: a review journal of the Institute of Mathematical Statistics* 30, 2 (2015), 199.
- [41] Peter Whittle. 1988. Restless bandits: Activity allocation in a changing world. *Journal of applied probability* 25, A (1988), 287–298.
- [42] Annie Xie, Logan Mondal Bhamidipati, Evan Zheran Liu, Joey Hong, Sergey Levine, and Chelsea Finn. 2024. Learning to Explore in POMDPs with Informational Rewards. In *Proceedings of the 41st International Conference on Machine Learning (Proceedings of Machine Learning Research, Vol. 235)*, Ruslan Salakhutdinov, Zico Kolter, Katherine Heller, Adrian Weller, Nuria Oliver, Jonathan Scarlett, and Felix Berkenkamp (Eds.). PMLR, 54414–54429. <https://proceedings.mlr.press/v235/>

A Summary of Related Work

We summarize the similarities and differences between our setting (in the “Latent-State” column) and existing settings in the literature in Table 4.

B Summary of Algorithms

We present the detailed description of the algorithms compared in Table 5.

C Proof of Theorem 1

Partition time into blocks of length τ . For simplicity assume τ divides T ; otherwise, the final incomplete block contributes an additional $O(1)$ term. There are T/τ probe rounds, hence the expected probe regret is at most $(T/\tau)\Delta_{\text{probe}}$.

Fix a block starting at t_0 (a probe time) and consider an offset $j = 1, \dots, \tau - 1$. If the state at time $t_0 + j$ differs from the state at t_0 , then the exploit arm chosen based on the probe at t_0 may be suboptimal at $t_0 + j$, incurring regret at most Δ_{max} . By a union

bound over the j transitions within the block,

$$\mathbb{P}(s_{t_0+j} \neq s_{t_0}) \leq \sum_{k=1}^j \mathbb{P}(s_{t_0+k} \neq s_{t_0+k-1}) \leq jq.$$

Therefore the expected staleness regret within this block is at most

$$\sum_{j=1}^{\tau-1} \Delta_{\text{max}} \mathbb{P}(s_{t_0+j} \neq s_{t_0}) \leq \Delta_{\text{max}} q \sum_{j=1}^{\tau-1} j = \frac{\Delta_{\text{max}} q}{2} \tau(\tau-1) \leq \frac{\Delta_{\text{max}} q}{2} \tau^2.$$

Summing over T/τ blocks yields a total staleness contribution at most $(\Delta_{\text{max}} q/2)\tau T$.

Finally, with probability at most ε_{fp} the probe at the start of a block returns the wrong optimal arm, in which case each of the next $\tau - 1$ exploitation steps can incur regret at most Δ_{max} . Thus the misclassification contribution is at most

$$\frac{T}{\tau} \cdot \varepsilon_{\text{fp}} \cdot \Delta_{\text{max}}(\tau - 1) \leq \Delta_{\text{max}} \varepsilon_{\text{fp}} \cdot T.$$

Dividing by T and accounting for the possible incomplete last block gives the stated bound.

Received 22 January 2026; revised 22 January 2026; accepted 22 January 2026

Feature	Classical	Contextual	Non-Stat.	Adversarial	Restless	RL / POMDP	LMDP	Latent-State
Stationarity	Yes	Yes	Arbitrary drift	Worst-case	Markovian	Markovian	Episodic	Markovian
State	None	Observable	N/A	None	Observable	Hidden/Partial	Hidden	Hidden
State Observability	N/A	Full	N/A	N/A	Observable	Partial	Hidden	Unobservable
Knowledge of Trans. Prob.	N/A	N/A	N/A	N/A	Known	Unknown/Learned	Unknown	Not modeled
Action Affects Transition	No	No	No	No	Yes	Yes	No	No
Trajectories Needed	Single	Single	Single	Single	Single	Multiple	Multiple	Single
Regret Type	Static	Contextual	Dynamic	Fixed	Index-based	Cumulative	Episodic	Dynamic

Table 4: Comparison of related work

Algorithm	Type	Key Mechanism
<i>Randomized Algorithms</i>		
AdaRP-UCB	Adaptive	Dual-component LinUCB with adaptive probing triggered by residual analysis, uncertainty gates, and hazard detection. Uses joint context features from synchronized probes and lagged individual contexts.
RP-UCB	Probing	Fixed-schedule probing every τ rounds with joint contextual features. Exploits with LinUCB using combined long-term (joint probe) and short-term (lagged) context information.
<i>Single-Unit Algorithms</i>		
AdaSP-UCB	Adaptive	Single-agent analog of AdaR-UCB with two-phase probing (consecutive arm sampling) triggered by the same adaptive gates: residual, uncertainty, and hazard.
LC-UCB	Contextual	Contextual LinUCB using previous reward and action as features. Constructs polynomial features with one-hot action encoding and interaction terms.
LC-TS	Contextual	Bayesian contextual Thompson Sampling with the same feature construction as LC-UCB. Maintains Gaussian posteriors per arm and samples from posterior distributions.
SP-UCB	Probing	Single-component version with fixed two-round probing cycle every τ steps, followed by LinUCB exploitation using synthetic joint context features.
D-UCB	Non-stationary	Discounted UCB with exponentially decaying arm statistics (γ discount factor) to handle non-stationarity through recency weighting.
SW-UCB	Non-stationary	Sliding window UCB maintaining fixed-size history of recent observations per arm, computing UCB bounds from windowed statistics only.
EXP3-S	Non-stationary	EXP3 variant with additive smoothing term in weight updates to improve performance in stochastic environments while maintaining adversarial guarantees.
UCB1	Classical	Standard upper confidence bound algorithm with $\sqrt{2 \ln t / N_a}$ exploration bonus. Maintains global arm statistics without adaptation.
TS	Classical	Thompson Sampling with independent Gaussian-Gamma conjugate priors per arm. Samples arm parameters from posterior distributions for decision making.
EXP3	Adversarial	Exponential weights algorithm mixing exploitation and uniform exploration. Updates weights using importance-weighted rewards with γ exploration parameter.
<i>Oracle Algorithms</i>		
Optimal Single Arm	Oracle	Theoretical baseline always selecting the arm with highest expected reward under the stationary distribution (uniform over states).

Table 5: Summary of Algorithms